Preprints of the 21st IFAC World Congress (Virtual)
Berlin, Germany, July 12-17, 2020

An Extremum Seeking Approach to Search and Rescue Operations in Avalanches using ARVA ⋆

Ilario A. Azzollini * **Nicola Mimmo** * **Lorenzo Marconi** *

* *CASY - DEI, University of Bologna, Italy*
(e-mail: {ilario.azzollini, nicola.mimmo2, lorenzo.marconi}@unibo.it).

Abstract: Search and rescue operations in avalanches can greatly benefit from the support of unmanned aerial vehicles, which could safely and autonomously fly above the snow surface to estimate the position of the victim. This work relies upon the Appareil de Recherche de Victimes (ARVA), which consists of a transmitter and a receiver. The transmitter is worn by the victim and produces an electromagnetic field that can be sensed by the receiver, integrated on the drone. A receiver able to sense the complete 3D electromagnetic field has been developed, whose model and properties are presented in this work. The main contribution of this work is the development of a control algorithm able to drive the ARVA-equipped drone as close as possible to the victim location.

Keywords: ARVA; Autonomous Robotic Systems; Extremum Seeking and Model Free Adaptive Control; Flying Robots; Search and Rescue.

1. INTRODUCTION

Future Search & Rescue (S&R) missions will exploit the support of robots more extensively in order to boost the efficiency of rescue operations while decreasing the risks associated to harsh environments (urban disasters, avalanches, earthquakes, etc.). Related to alpine environment, (Cacace et al., 2016b,a; Bevacqua et al., 2015) demonstrated how S&R operations can greatly benefit from the use of autonomous Unmanned Aerial Vehicles (UAVs) to survey the environment and collect evidences about the position of a missing person. In particular, the European projects *SHERPA* (Marconi et al., 2012) and *AirBorne* (Air, 2018) address a specific challenge in S&R robotics: the establishment of an effective solution to support professional alpine rescue teams in avalanche scenarios.

The rescue missions in avalanche are characterized by specific peculiarities that make common S&R technologies and practices not efficient. One of the most important aspects is the rescue time: the survival chances of people buried under the snow decreases rapidly with burial time due to hypothermia. Secondly, the harshness of the rescue scene is represented by irregular and unstable snow blocks usually on steep slopes. Finally, a limited range of sensors can be used to localize a person buried under the snow (Ferrara, 2015). One of the most common tools is the so called ARVA system. The system ARVA consists of two elements: a *transmitter* and a *receiver*. The transmitter is worn by the avalanche victims and emits a signal detectable by the receiver, which is held by the rescuers. The receiver provides information about the electromagnetic field generated by the transmitter sensed at the receiver location. The rescuers are trained to interpret these data to move towards the victim. Unfortunately, this technique requires a non-negligible amount of time, period during which the rescuers walk on the unstable avalanche snow, with the tangible risk of inducing a second avalanche event. In this context, drones represent a valid support for humans. Indeed, if sufficiently smart, ARVA-driven drones can fly autonomously above the snow to find the transmitter location, thus resulting in faster and safer search.

The search technique currently adopted by the rescuers consists in approaching the transmitter by walking on the path defined by the ARVA ElectroMagnetic (EM) flux lines, sensed at the receiver location. Instead, to enable fast and reliable UAV-based S&R, we propose in this work an alternative search strategy based on the signal strength. In detail, the proposed approach belongs to the class of the so-called *source seeking* control problems. In the framework of the source seeking, the agent senses the signal emitted by an omni-directional source located at an unknown position. Thanks to the knowledge of this signal, the control aims to steer the agent towards the source. Several approaches have been developed to solve this class of control problems with remarkable examples constituted by (Cochran and Krstic, 2007; Cochran et al., 2007, 2008), in which the *Extremum Seeking* (ES) control paradigm has been exploited to provide the solution in absence of a detailed output map. Furthermore, (Mayhew et al., 2008) provided a control strategy inspired by a *line minimization-based algorithm* for unconstrained optimization of nonlinear functions without gradient information, whereas (Mellucci et al., 2016) proposed a gradient-free control law (a sliding mode controller solving a *boundary tracking problem*) which exploits local measurements of the phenomenon at the vehicle's position only.

All the examples available in literature of UAVs equipped with the ARVA technology belong to source seeking approach (Bregu et al., 2016; Silvagni et al., 2017; Grauwiler and Oth, 2010). In these works, the UAVs are equipped with receivers based on a single antenna and thus able to sense the EM field only in one direction. As a consequence, the performance of these systems are constrained by the selected technology. On the other hand, one of the main goals of the project AirBorne regards the development of an UAV equipped with an ARVA receiver constituted by three orthogonal antennas, thus able to

⋆ This research was supported by the European Project "AerIal RoBotic technologies for professiOnal seaRch aNd rescuE" (AirBorne), Call: H2020, ICT-25-2016/17, Grant Agreement no: 780960.

sense the complete 3D EM field. The future availability of such a receiver will lead to a revolution in the search techniques and, in this context, this paper introduces the following novelties. First, the 3D ARVA system is presented in detail, as well as the properties of the signal. Then, a solution to the AirBorne S&R problem is proposed, based on ES. This solution is promising for two main reasons: (i) being an approximate gradient-based optimization technique, it can highly improve on the flux lines-based search; (ii) ES control systems are intrinsically robust due to their model-free nature.

This paper is organized ad follows. Section 2 introduces the preliminaries, followed by the problem formulation in Section 3. In Section 4 the ARVA system is presented, while the proposed solution is described in Section 5. Finally, numerical simulations are shown in Section 6 and the conclusions are presented in Section 7.

2. PRELIMINARIES

The transpose of a real-valued vector or matrix is denoted by $(\cdot)^\top$. The symbols $\mathbb{R}$, $\mathbb{R}_>$, $\mathbb{R}_\geq$ denote the set of real, positive real, and non-negative real numbers, respectively. $I_n \in \mathbb{R}^{n\times n}$ is used to denote the n-dimensional identity matrix, while $0_{n\times m}$ denotes a $n \times m$ matrix of zeros. With $SO(3)$ it is denoted the *special orthogonal group* of 3D rotation matrices, i.e. $SO(3) = \{R \in \mathbb{R}^{3\times 3} : R^\top R = RR^\top = I_3, \det R = 1\}$. For a differentiable function g, its gradient is denoted by Dg, while $D^2 g = D(Dg)$ denotes its Hessian.

In this manuscript, three Cartesian coordinate frames are defined: $\mathcal{F}_i = (\mathrm{O}_i, x_i, y_i, z_i)$ indicates the right-handed static inertial frame, while $\mathcal{F}_t = (O_t, x_t, y_t, z_t)$ and $\mathcal{F}_r = (\mathrm{O}_r, x_r, y_r, z_r)$ are the right-handed frames associated to the static transmitter worn by the victim and to the receiver installed on the moving drone, respectively. The positions of O_r and O_t relative to O_i are indicated by the vectors $p_r \in \mathbb{R}^3$ and $p_t \in \mathbb{R}^3$, respectively. Given that O_t and O_i are static reference frames, p_t is a constant. The position of O_r relative to O_t is indicated by the vector $p \in \mathbb{R}^3$, with $p = p_r - p_t$. Throughout the paper, we shall use the superscripts i, t and r on the left of the vectors p, p_t, p_r to denote the representation of the previous vectors in the reference frames $\mathcal{F}_i$, $\mathcal{F}_t$ and $\mathcal{F}_r$, respectively (for instance, ${}^i p$ denotes a representation of p in $\mathcal{F}_i$). The orientation of the $\#$-frame $\mathcal{F}_\#$ with respect to the inertial frame $\mathcal{F}_i$ is expressed by means of the rotation matrix ${}^i R_\# \in SO(3)$ (from the $\#$-frame to the inertial frame). In the following, either $\# = r$ when dealing with the drone-receiver frame, or $\# = t$ for the victim-transmitter frame. Finally, let a generic position with respect to the inertial frame be given by ${}^i P = [{}^i x \ {}^i y \ {}^i z]^\top$.

2.1 Brief Introduction about Extremum Seeking Control

ES is a form of adaptive control where the steady-state input-output characteristic is optimized, without requiring any explicit knowledge about this input-output map other than it is static and it has an extremum (Ariyur and Krstic, 2003; Tan et al., 2006, 2010). For simplicity, let us consider a single-input single-output system as in Figure 1. In particular, let the plant dynamics be modeled as

$$\dot{x} = f(x, u), \quad y = h(x), \tag{1}$$

where $x \in \mathbb{R}^n$ is the internal state, $u \in \mathbb{R}$ is the input, $y \in \mathbb{R}$ is the measurable output, and the functions f, h are assumed to be differentiable in their arguments. Assuming

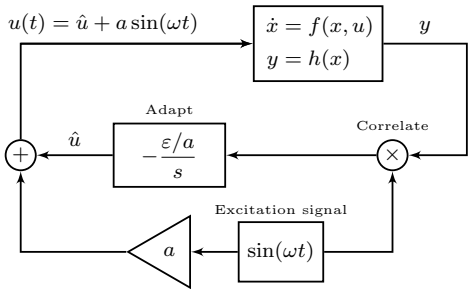

Fig. 1. Extremum seeking control scheme (Tan et al., 2010).

that the Steady-State Characteristic (SSC) has a minimum, the control objective is to drive the input-output pair (u, y_p) to the extremum (u^*, y_p^*). The following assumptions are needed.

Assumption 1. (Tan et al., 2010) There exists a (differentiable) function $l : \mathbb{R} \to \mathbb{R}^n$ such that

$$f(x, u) = 0 \quad \text{iff} \quad x = l(u).$$

Assumption 2. (Tan et al., 2010) For each constant u, the corresponding equilibrium $x = l(u)$ of system (1) is globally asymptotically stable, uniformly in u.

Assumption 3. (Tan et al., 2010) Consider l defined as in Assumption 2. Let $g(u) = h(l(u))$ be the steady-state characteristic. There exists a unique u^* minimizing g:

$$Dg(u^*) = 0, \qquad D^2 g(u^*) > 0$$
$$Dg(u^* + \zeta)\zeta > 0, \quad \forall \zeta \in \mathbb{R} \neq 0.$$

Assumption 1 ensures that the SSC is well defined and given by a differentiable function, while Assumption 2 ensures that this SSC is stable, attractive and unique (uniformly in u). Finally, Assumption 3 guarantees that the SSC has a unique minimum. The control scheme shown in Figure 1 achieves extremum seeking in a practical way ((u, y) converge to a neighborhood of (u^*, y^*)) if the parameters of the controller are appropriately adjusted as to guarantee the following time scale separation:

(1) *Fast time variations*: the x-dynamics quickly settle down to a neighborhood of the equilibrium manifold $x(t) = l(u) = l(\hat{u} + a\sin(\omega t))$;
(2) *Intermediate time variations*: through the excitation signal $a\sin(\omega t)$, a neighborhood of the equilibrium manifold around the present estimate $\hat{u}$ is explored;
(3) *Slow time variations*: the learning dynamics, with $\omega \gg \epsilon > 0$, and $a > 0$ sufficiently small (much smaller than the expected $|u^*|$), $\hat{u}$ slowly evolves in the gradient-descent direction $-Dg(\hat{u})$ to seek the minimizer u^*.

The work (Tan et al., 2006) proved semi-global practical stability of the closed-loop system with respect to the design parameters. Finally, when there is more than one parameter to be optimized (multi-input single-output case), as a generalization of Assumption 3, the SSC function is required to be *unimodal*. The multi-parameter ES control scheme can be found in (Ariyur and Krstic, 2003, Chapter 2).

Definition 1. (Unimodal Function). A function g is unimodal if:

- The domain $\mathrm{dom}(g)$ is a convex set;
- There exists an optimal solution $u^* \in \mathrm{dom}(g)$ such that $g(u^*) \leq g(u)$ for all $u \in \mathrm{dom}(g)$;
- For all $u_0 \in \mathrm{dom}(g)$, there exists a trajectory $u(\lambda) \in \mathrm{dom}(g)$, with $u(0) = u_0$ and $u(1) = u^*$ such that $g\big(u(\lambda)\big) \leq g(u_0)$ for all $\lambda \in [0, 1]$.

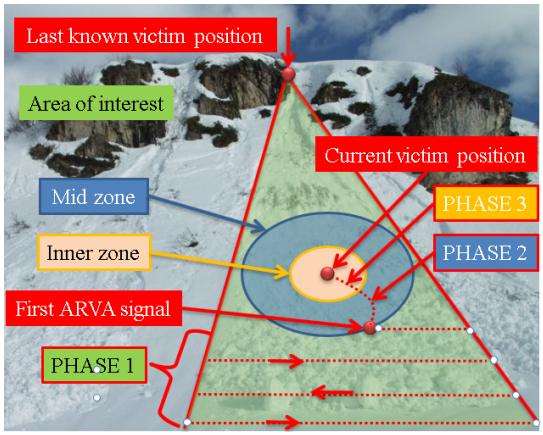

Fig. 2. Rescue scene: area of interest and search phases.

3. STATE OF THE ART AND PROBLEM FORMULATION

The transceivers commercially available have two operating modes, namely they can work as receivers or as transmitters, with a manual switch used to commute between the two modes. The ARVA system is based on the emission and sensing of an EM field. In details, the transmitter emits a signal which is sensed, elaborated and made available for the user by the receiver. Before starting their activities, experienced skiers switch the worn sensor to the transmitter mode. In case of an accident, companions not buried by the avalanche, or rescuers who reach the disaster area, switch their devices to the receiver mode and start searching the victim by following the standard ARVA-based four-steps strategy.

The *first search phase* starts with the definition of the area of interest in which the operators should find the victim. Typical scenarios are similar to what shown in Figure 2, where a triangular area departs from the last known victim position and includes the avalanche front.

Primary search (looking for a valid signal): The strength of the EM field sensed by the receiver is inversely proportional to the Euclidean distance between the receiver and the transmitter. When this distance is too long, the receiver is unable to recognize the EM field and does not display information to the operator. Thus, in the first phase of the search the rescuers scan the area to find a valid ARVA signal. Usually the first search is done by following straight parallel lines with an offset of 15-20 meters. It is worth noticing that the search starts from the bottom because, since the avalanche drags people downstream, the valley represents the area with the highest probability of burials.

Secondary search (flux lines search): If sufficiently close to the transmitter (typically around 50 meters), the commercial ARVA receivers display the EM field vector in terms of magnitude and direction, sensed at the receiver location and expressed in the $\mathcal{F}_r$ frame. This information actually corresponds to the tangent to the EM field flux line at the operator location. Since the flux lines converge to the transmitter, the rescuers follow the flux line to approach the victim. Unfortunately, this strategy has some drawbacks: (i) the search path can be unpredictably long as it depends on the initial position of the receiver with respect to the transmitter; (ii) the search path depends on the initial receiver attitude with respect to the transmitter (the rescuers could follow the flux lines counterclockwise or clockwise thus leading to different search paths); (iii) any strategy for the inversion of the motion based on the local estimation of the distance gradient should be sufficiently robust to avoid to fall in local minima (due to the environment EM noise); (iv) if the transmitter is not on the search plane (practically always due to the burial depth), the flux lines-based search leads to a couple of local minima which do not correspond to the point on the search plane at minimum distance from the transmitter.

Tertiary search (pinpointing): When the sensed EM field is sufficiently strong, the commercial ARVA receivers change their output modality and provide only the modulus of the EM field at the operator location. This change of modality informs the rescuers that the flux line approach is no more efficient and that a new search approach, based on the maximization of the intensity of the signal, is necessary. Usually, rescuers determine the victim location somehow iterating the following two–steps gradient search: (i) find the maximum intensity on an initial straight line; (ii) find the maximum intensity on a second straight line, perpendicular to the previous one and passing through the previous maximum.

In the context of the project AirBorne, this paper aims at the design of a control law which guides an autonomous flying robotic platform, equipped with an ARVA receiver, to support and possibly improve the search operations. First of all, the creation of a collaborative robotic tool, supporting the rescuers without obstructing them during the field operations, requires the safe co-existence of humans and drones on the avalanche site. The simplest way to fulfill this requirement consists in the introduction of a vertical separation between rescuers and robots. In particular, considering the $x_i y_i$-plane (with ${}^i z = 0$) of the inertial frame $\mathcal{F}_i$ as corresponding to the snow surface, the drone will be required to operate on a parallel plane having ${}^i z \geq 4$ m. Intuitively, in this framework the victim-transmitter location expressed in the inertial frame ${}^i p_t$ will have a negative component along the z_i-axis (as it is buried under the snow surface).

Problem 1. Assume that the first and the second search phases are left in charge of the expert rescuers, which are called to defined the search area, and suitable coverage algorithms to optimize the initial scan of the area. Also assume that the drone initial position is on a desired search plane where a valid ARVA signal was found by the drone. Design a control law, based on extremum seeking, such that the drone is autonomously driven as close as possible to the victim-transmitter position, even though constrained to fly on the defined search plane. The problem needs to be solved in a stable and robust way both with respect to the EM noise, and without using the exact model of the ARVA function, thus resulting in a practically implementable control algorithm.

4. CHARACTERIZATION OF THE ARVA SYSTEM

The ARVA system relies on a *transmitter* device that generates a magnetic field which is modeled as a dipole aligned with the x_t axis of $\mathcal{F}_t$. The electromagnetic vector field, described in $\mathcal{F}_i$, is indicated by ${}^i h \in \mathbb{R}^3$. Let ${}^i p = [x\ y\ z]^\top$, it turns out that a mathematical model of the magnetic vector field is given by (Piniés and Tardós, 2006)

$$ {}^i h({}^i p, {}^i R_t) = \frac{1}{4\pi \| {}^i p \|^5} \mathrm{A}({}^i p)\, {}^i R_t e_1 \qquad (2) $$

where

$$\mathrm{A}(p) := \begin{bmatrix} 2x^2 - y^2 - z^2 & 3xy & 3xz \\ 3xy & 2y^2 - x^2 - z^2 & 3yz \\ 3xz & 3yz & 2z^2 - x^2 - y^2 \end{bmatrix}$$

and $e_1 = [1\ 0\ 0]^\top$. The intensity of the magnetic field can be then obtained by the previous relation as (Piniés and Tardós, 2006)

$$\| {}^i h\| = \frac{1}{4\pi \| {}^i p\|^3} \sqrt{1 + 3 \frac{{}^i p^\top M\, {}^i p}{\| {}^i p\|^2}} \tag{3}$$

where $M = {}^t R_i^\top e_1 e_1^\top {}^t R_i \geq 0$ with minimum and maximum singular values given by $\underline{\sigma}(M) = 0$ and $\overline{\sigma}(M) = 1$, respectively. The flux lines described by (2) are symmetric with respect to the transmitter x_t-axis. Furthermore, (3) can be exploited to compute the iso–power lines which are also symmetric with respect to the transmitter x_t-axis.

The ARVA equipment has three antennas directed along the *receiver* frame axes x_r, y_r and z_r, namely along the longitudinal, lateral and vertical direction of the sensor case. The magnetic field sensed at the receiver location, denoted by ${}^i h_m$, is given by

$${}^i h_m({}^i p, {}^i R_t, t) = {}^i h({}^i p, {}^i R_t) + {}^i w(t) \tag{4}$$

where ${}^i w(t) : \mathbb{R} \mapsto \mathbb{R}^3$ indicates the electromagnetic interfenence expressed in the inertial frame. This noise is bounded by $\| {}^i w\|_\infty \leq \bar{w} \in \mathbb{R}_>$. It is worth observing that the ARVA measurement, ${}^i h_m$, is bounded from below by $\bar{w}$ but it is not bounded from above as

$$\lim_{\| {}^i p\| \to \infty} \| {}^i h_m\|_\infty = \bar{w}, \qquad \lim_{\| {}^i p\| \to 0} \| {}^i h_m\|_\infty = \infty. \tag{5}$$

As a consequence, any algorithm based on the gradient descent directly exploiting ${}^i h_m$ would face with issues in the proximity of the victim. This criticism motivates the manipulation of the ARVA measurement described in Section 5.

5. THE PROPOSED SOLUTION

The ARVA output ${}^i h_m$ is elaborated to create a map which is continuous and bounded for any ${}^i p \in \mathbb{R}^3$. In detail, the following nonlinear function is used

$$y_t({}^i p, {}^i R_t, t) := \| {}^i h_m\|^{-1/3} \approx {}^i h_{\mathrm{n}}({}^i p, {}^i R_t) + \nu_t({}^i p, {}^i R_t, t) \tag{6}$$

in which the nominal field is identified by the term

$${}^i h_{\mathrm{n}}({}^i p, {}^i R_t) = \frac{(4\pi)^{1/3} \| {}^i p\|}{\sqrt[6]{1 + 3 \dfrac{{}^i p^\top M\, {}^i p}{\| {}^i p\|^2}}} \tag{7}$$

whereas the equivalent additive noise is given by

$$\nu_t({}^i p, {}^i R_t, t) = \left. \frac{\partial \| {}^i h_m\|^{-1/3}}{\partial\, {}^i w} \right|_{{}^i w = 0} {}^i w(t) \tag{8}$$

where

$$\left. \frac{\partial \| {}^i h_m\|^{-1/3}}{\partial\, {}^i w} \right|_{{}^i w = 0} = \nabla_A({}^i p, {}^i R_t) \| {}^i p\|^3 \tag{9}$$

with $\nabla_A({}^i p, {}^i R_t) \in \mathbb{R}^3$ bounded.

The new output map (6) shows some interesting properties. First, it is well defined because for any ${}^i p \in \mathbb{R}^3$

$$0 \leq \frac{{}^i p^\top M\, {}^i p}{\| {}^i p\|^2} \leq 1. \tag{10}$$

Secondly, for any fixed ${}^i R_t \in SO(3)$ and $t > 0$ the functions ${}^i h_{\mathrm{n}}(\cdot, {}^i R_t), \nu_t(\cdot, {}^i R_t, t) \in \mathcal{K}_\infty$ and thus have a global minimum at ${}^i p = 0$.

A further important property of the function (6) is relative to the Noise-to-Signal Ratio (NSR). Since both ${}^i h_{\mathrm{n}}(\cdot, {}^i R_t)$ and $\nu_t(\cdot, {}^i R_t, t)$ belong to $\mathcal{K}_\infty$ the standard NSR, namely $\|\nu_t(\cdot, {}^i R_t, t)\|_\infty / |{}^i h_{\mathrm{n}}(\cdot, {}^i R_t)|$, results to be not bounded. Thus, the NSR is evaluated by means of the modified bounded ratio

$$\overline{\mathrm{NSR}}({}^i p, {}^i R_t) = \frac{\|y_t({}^i p, {}^i R_t, t)\|_\infty - |{}^i h_{\mathrm{n}}({}^i p, {}^i R_t)|}{\|y_t({}^i p, {}^i R_t, t)\|_\infty}. \tag{11}$$

This modified ratio belongs to the compact domain $[0,\ 1]$ and, in particular, for any ${}^i R_t \in SO(3)$

$$\lim_{{}^i p \to 0} \overline{\mathrm{NSR}}({}^i p, {}^i R_t) = 0, \qquad \lim_{{}^i p \to \infty} \overline{\mathrm{NSR}}({}^i p, {}^i R_t) = 1 \tag{12}$$

meaning that at the origin ${}^i p = 0$ the output is not affected by noise whereas for ${}^i p \to \infty$ the nominal signal is annihilated by the noise.

Remark 1. Considering Problem 1, it is assumed that the NSR is favorable from the start of the automatic search, as the ARVA receiver is able to tell the user whether the signal is valid or not. Recall that the first two search phases are assumed to be already completed. It is worth remarking that, even if the noise ν_t is highly correlated with the receiver movement (in particular its position), the resulting elaborated ARVA output function y_t preserves the $\mathcal{K}_\infty$ property and preserves the minimum at ${}^i p = 0$. In conclusion, this function is unimodal and can be optimized by means of ES.

Let the victim-transmitter be located at a certain unknown (static) position ${}^i p_t$ with an unknown (static) orientation given by ${}^i R_t$. The elaborated ARVA function basically maps from the drone-receiver position ${}^i p_r$ to the output y_t, as there is no control on the transmitter-related quantities. Therefore, in the context of ES control there are three inputs: the components of ${}^i p_r$, which can be "moved". Given the assumption that the automatic search starts from a position close enough to the victim such that the ARVA signal is valid, ES could be directly used to solve the 3D problem. However, everything needs to be specialized for the given search plane, as a 3D search cannot be performed (see Problem 1). Let ${}^i p_{r/s} = [{}^i x_d\ {}^i y_d\ {}^i z_d = z^*]^\top$ be the position of the drone-receiver constrained on the search plane described by ${}^i z = z^*$, while let the (static) position of the victim-transmitter be denoted by ${}^i p_t = [{}^i x_v\ {}^i y_v\ {}^i z_v]^\top$. As a consequence, the constrained distance ${}^i p_{/s} := {}^i p_{r/s} - {}^i p_t$ is defined. It can be demonstrated that also $y_t({}^i p_{/s}, {}^i R_t)$ is unimodal, having a unique global minimum. Therefore, ES can be used also in the context of this 2D search, with inputs $({}^i x_d, {}^i y_d)$.

Remark 2. The geometric projection of the victim position on the search plane is simply $[{}^i x_v\ {}^i y_v\ \ {}^i z = z^*]^\top$. It is worth remarking that this does not necessarily correspond to the position of the minimum of the constrained ARVA function $y_t({}^i p_{/s}, {}^i R_t)$, unless, either ${}^i R_t = I_3$ or the victim is exactly on the search plane. When the transmitter has a different orientation with respect to the inertial frame and the victim is not located at ${}^i z = z^*$, the optimal position on the search plane will only be in a neighborhood of $[{}^i x_v\ {}^i y_v\ {}^i z = z^*]^\top$ which depends both on ${}^i R_t$ and on the distance between the search plane and the position of the victim $z^* - {}^i z_v$. Intuitively, given

a certain orientation ${}^iR_t$, the distance between the optimal position on the search plane and the geometric projection of the victim position on the search plane increases with the distance $z^* - {}^iz_v$. It will be commented in numerical simulations why this result is more than acceptable.

The control scheme proposed to solve Problem 1 is shown in Figure 3. It is made of two blocks working in synergy.

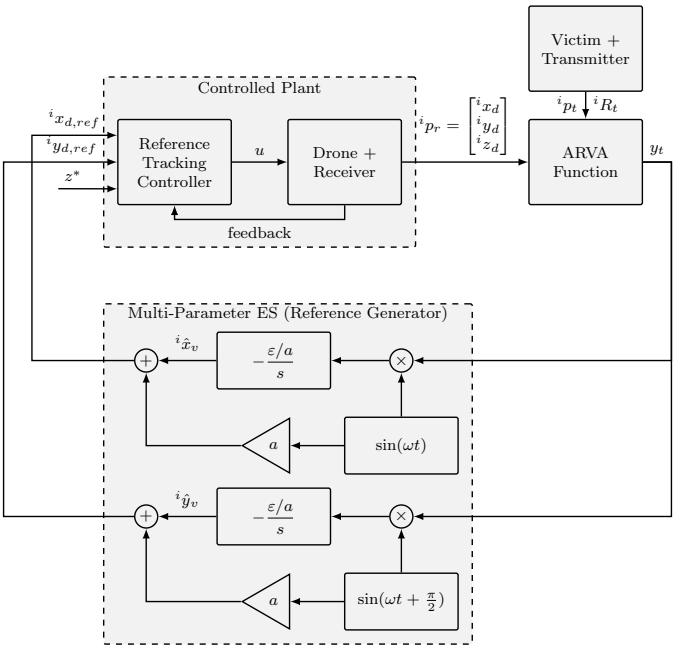

Fig. 3. Overall control scheme.

Multi-Parameter Extremum Seeking (Reference Generator) This block processes the ARVA elaborated output y_t, and its role is that of driving the parameters $({}^ix_d, {}^iy_d)$ to the optimal ones corresponding to the minimum of the constrained ARVA function $y_t({}^ip_{/s}, {}^iR_t)$. Due to the time scale separation, the ES design can be made by considering the Controlled Plant of Figure 3 as a static system. The search of the minimum on the plane ${}^iz = z^*$ is a multi-parameter ES problem in which, multiple inputs $({}^ix_d, {}^iy_d)$ are exploited to optimize a single output (y_t). Taking (Ariyur and Krstic, 2003, Chapter 2) as reference, it is enough to have as many ES optimization channels as the number of inputs/parameters. The excitation signals should be carefully designed, in order to guarantee proper exploration of the parameters space. In this particular case, as we have two parameters to estimate, the same frequency ω can be chosen for the excitation signals. We choose to shift the sinusoid of the second channel (${}^iy_d$ channel) by $\pi/2$: in this way we are exploring the search plane by moving in circular trajectories of radius a, which is a smooth trajectory that can be easily tracked by a UAV. The parameters a, ω, and ϵ can be designed so as to make the extremum seeking scheme as fast as possible, both considering the maximum allowed speed for the UAV and respecting the recommendations of Subsection 2.1.

Reference Tracking Controller (RTC) Given the height reference z^* and the references generated from the ES, this controller aims to drive the drone position ${}^ip_r$ to the references as fast as possible, so as to ensure the time scale separation needed for the proper functioning of ES. The details of the designed RTC are omitted for lack of space and are left to a forthcoming work.

6. NUMERICAL SIMULATIONS

Recalling Problem 1, as a starting point for this numerical example let us consider the drone-receiver to be located at ${}^ip_r = [{}^ix_d = 0 \ {}^iy_d = 0 \ {}^iz_d = z^* = 5]^\top$, corresponding to the position in space where the first ARVA signal has been available after the *primary search*. As a consequence, the initial distance between the drone and the transmitter is approximately 50 meters. In particular, for the results shown in Figure 4, the victim location is ${}^ip_t = [{}^ix_v = -27.6 \ {}^iy_v = 41.1 \ {}^iz_v = -10]^\top$. Moreover, the (unknown) orientation of the transmitter, given by ${}^iR_t$, was numerically chosen so as to obtain a worst case scenario in terms of the distance between the optimal position on the search plane ${}^iz = z^*$ and the geometric projection of the victim position on the search plane (which in this particular case is $[-27.6 \ \ 41.1 \ \ 5]^\top$). The ES design parameters were chosen in order to perform the search as fast as possible by ensuring that the drone velocity never exceeded 5 m/s, in particular: $a = 5$, $\omega = 0.65$, and $\epsilon = 0.3$.

In order to comment on the results, it is worth noticing that the research is divided in two different phases. In fact, referring to Figure 4-(g), we see that the drone is first finding the optimal position on the ${}^iz = 5$-plane, and then after 300 seconds, when the changes in the function value y_t are not significant anymore (see Figure 4-(h)), the search plane is shifted to ${}^iz = 0.5$ in order to obtain a better estimate. As a matter of fact, in agreement with Remark 2 this strategy improves the estimation, as depicted in Figures 4-(b),(e),(h). Figures 4-(a),(d),(i) show how the designed oscillatory behavior on both ${}^ix_d$ and ${}^iy_d$ generates circular trajectories of radius a on the search plane. Figures 4-(c),(f) show the tracking performance guaranteed by the RTC: tracking is fast enough to guarantee the proper time scale separation for the chosen ES parameters.

The final outcome is that, after the first search performed on a plane at a 15 meters distance from the victim, the optimal position found is $[-24.3 \ \ 39.5 \ \ 5]^\top$, which is only at a 3.7 meters distance from the geometric projection $[-27.6 \ 41.1 \ 5]^\top$. This is testified also by Figures 4-(a),(d), where it is clear that even before $t = 300s$ the drone is already oscillating around $({}^ix_v, {}^iy_v)$. This result is of great practical importance because, as victims are usually buried between 0.5 and 10 meters under the level of the snow, the performed simulation represents a worst case scenario. Moreover, the people in charge of the last part of the rescue operation involving digging and finding the victim, are very well trained and able to quickly save the victim if they are given an estimate $({}^i\hat{x}_v, {}^i\hat{y}_v)$ which is located in a 10 meters radius from the real one. For this reason, the accuracy of 3.7 meters, obtained in the worst case, indicates that the ES approach can be a realistic solution to Problem 1.

7. CONCLUSIONS

In this work, the presented S&R problem for a single victim was solved by means of an autonomous UAV equipped with an ARVA receiver. In particular, extremum seeking control was proven to be efficient in speeding up the third search phase of the rescue operations. Future work will be devoted to bring the presented algorithm on the field for experimental tests.

REFERENCES

(2018). AerIal RoBotic technologies for professiOnal seaRch aNd rescuE. URL https://www.airborne-project.eu/.

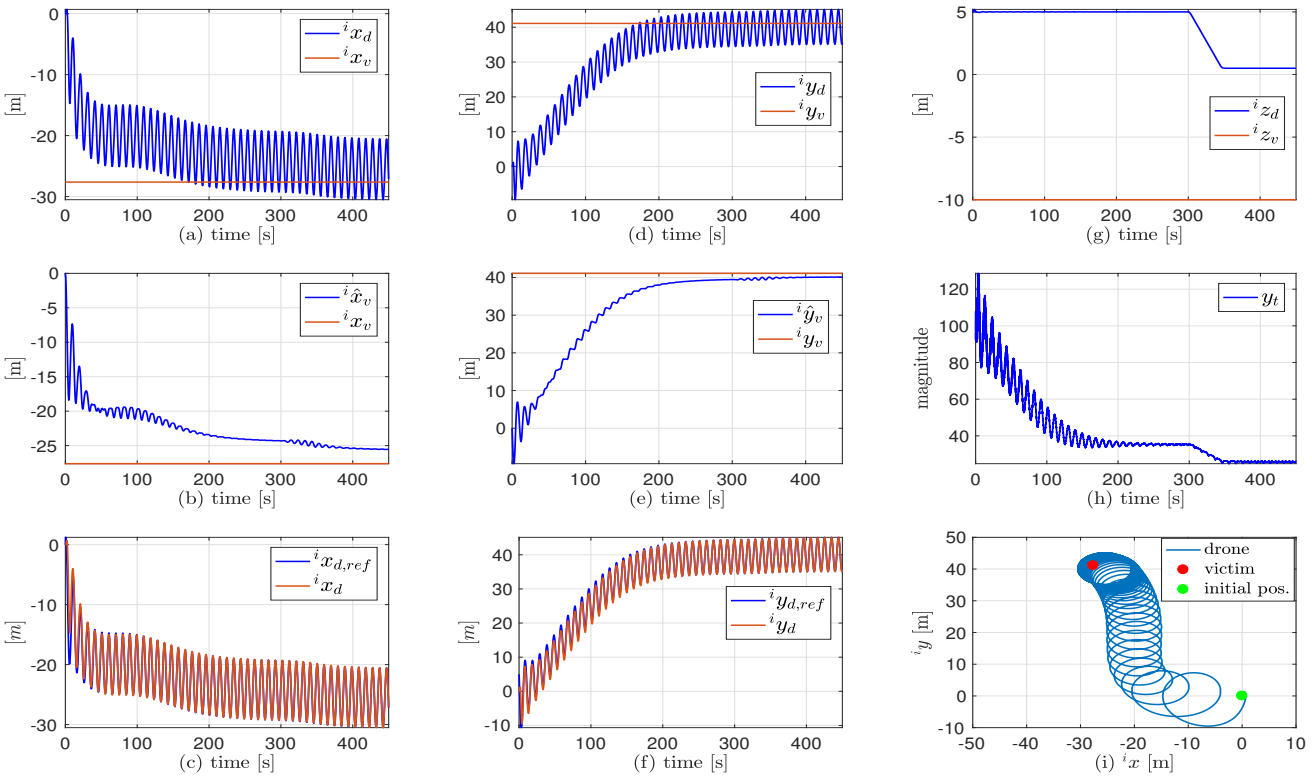

Fig. 4. Results of the numerical simulation.

Ariyur, K.B. and Krstic, M. (2003). *Real-time optimization by extremum-seeking control*. John Wiley & Sons.

Bevacqua, G., Cacace, J., Finzi, A., and Lippiello, V. (2015). Mixed-initiative planning and execution for multiple drones in search and rescue missions. In *Twenty-Fifth International Conference on Automated Planning and Scheduling*.

Bregu, E., Casamassima, N., Cantoni, D., Mottola, L., and Whitehouse, K. (2016). Reactive control of autonomous drones. In *Proceedings of the 14th Annual International Conference on Mobile Systems, Applications, and Services*, 207–219. ACM.

Cacace, J., Finzi, A., and Lippiello, V. (2016a). Implicit robot selection for human multi-robot interaction in search and rescue missions. In *2016 25th IEEE International Symposium on Robot and Human Interactive Communication (RO-MAN)*, 803–808.

Cacace, J., Finzi, A., Lippiello, V., Furci, M., Mimmo, N., and Marconi, L. (2016b). A control architecture for multiple drones operated via multimodal interaction in search & rescue mission. In *2016 IEEE International Symposium on Safety, Security, and Rescue Robotics (SSRR)*, 233–239.

Cochran, J., Ghods, N., and Krstic, M. (2008). 3d nonholonomic source seeking without position measurement. In *2008 American Control Conference*, 3518–3523.

Cochran, J. and Krstic, M. (2007). Source seeking with a nonholonomic unicycle without position measurements and with tuning of angular velocity part i: Stability analysis. In *2007 46th IEEE Conference on Decision and Control*, 6009–6016.

Cochran, J., Siranosian, A., Ghods, N., and Krstic, M. (2007). Source seeking with a nonholonomic unicycle without position measurements and with tuning of angular velocity—part ii: Applications. In *2007 46th IEEE Conference on Decision and Control*, 1951–1956.

Ferrara, V. (2015). Technical survey about available technologies for detecting buried people under rubble or avalanches. *WIT Transactions on The Built Environment*, 150, 91–101.

Grauwiler, M. and Oth, L. (2010). Alcedo–the flying avalanche transceiver. *Zurich: European Satellite Navigation Competition*.

Marconi, L., Melchiorri, C., Beetz, M., Pangercic, D., Siegwart, R., Leutenegger, S., Carloni, R., Stramigioli, S., Bruyninckx, H., Doherty, P., et al. (2012). The sherpa project: Smart collaboration between humans and ground-aerial robots for improving rescuing activities in alpine environments. In *2012 IEEE International Symposium on Safety, Security, and Rescue Robotics (SSRR)*, 1–4.

Mayhew, C.G., Sanfelice, R.G., and Teel, A.R. (2008). Robust source-seeking hybrid controllers for nonholonomic vehicles. In *2008 American Control Conference*, 2722–2727.

Mellucci, C., Menon, P.P., Edwards, C., and Challenor, P. (2016). Source seeking using a single autonomous vehicle. In *2016 American Control Conference (ACC)*, 6441–6446.

Piniés, P. and Tardós, J.D. (2006). Fast localization of avalanche victims using sum of gaussians. In *Proceedings 2006 IEEE International Conference on Robotics and Automation, 2006. ICRA 2006.*, 3989–3994.

Silvagni, M., Tonoli, A., Zenerino, E., and Chiaberge, M. (2017). Multipurpose uav for search and rescue operations in mountain avalanche events. *Geomatics, Natural Hazards and Risk*, 8(1), 18–33.

Tan, Y., Moase, W.H., Manzie, C., Nešić, D., and Mareels, I. (2010). Extremum seeking from 1922 to 2010. In *Proceedings of the 29th Chinese Control Conference*, 14–26.

Tan, Y., Nešić, D., and Mareels, I. (2006). On non-local stability properties of extremum seeking control. *Automatica*, 42(6), 889–903.